[1]W.R. Bennett, Jr., G.N. Mercer, P.J. Kindlmann, B. Wexler, and H. Hyman, Phys. Rev. Letters **17**, 987 (1966).

[2]J.M. Hammer and C.P. Wen, J. Chem. Phys. **46**, 1225 (1967).

[3]O. Fisher, Z. Physik **86**, 646 (1933).

[4]P.N. Clout and D.W.O. Heddle, *Proceedings of the Sixth International Conference on the Physics of Electronic and Atomic Collisions, Cambridge, Mass.* (MIT Press, Cambridge 1969), p. 290.

[5]J.D. Jobe and R.M. St. John, Phys. Rev. **164**, 117 (1967).

[6]C.E. Moore, *Atomic Energy Levels*, Natl. Bur. Std. (U.S.) (GPO, Washington, D.C., 1949), Circular 467,Vol. 1.

[7]L. Minnhagen, Arkiv Fysik **25**, 203 (1963).

[8]J.C. DeVos, Physica **20**, 690 (1954).

[9]D. Rapp and P. Englander-Golden, J. Chem. Phys. **43**, 1464 (1965).

[10]J.R. Schumaker and C.H. Popenoe, J. Opt. Soc. Am. **59**, 980 (1969).

[11]R.I. Rudko and C.L. Tang, J. Appl. Phys. **38**, 4731 (1967).

[12]S.H. Koozekanani, IEEE J. Quantum Electron. QE-2, 770 (1966).

[13]H.R. Moustafa Moussa and F.J. DeHeer, Physica **36**, 646 (1967).

[14]F. Fiquet-Fayard, J. Chim. Phys. **62**, 1065 (1965).

[15]S.H. Koozekanani, IEEE J. Quantum Electron. Letters QE-3, 206 (1967).

[16]W.R. Bennett, Jr., J.W. Kuntson, Jr., G.N. Mercer, and J.L. Detch, Appl. Phys. Letters **4**, 180 (1964).

Absolute Fluorescence Yields of 3914-Å Photons from N_2 and Air Excited by Relativistic Electrons*

M. N. Hirsh, E. Poss, and P. N. Eisner

The Dewey Electronics Corporation, New York, New York 10016

(Received 26 September 1969)

The absolute fluorescence intensity of the first negative (0, 0) band of N_2^+ at 3914 Å excited by bombardment of N_2 and N_2:O_2 mixtures with electrons in the previously unstudied energy range 0.65 to 1.6 MeV has been measured at gas pressures of 0.05 to 8 Torr. An effective cross section for the production of these photons by 1.5-MeV primary electrons and all secondary electrons resulting from the ionization events is found to be $(1.6 \pm 0.4) \times 10^{-19}$ cm^2. The measurements indicate that 10% of the N_2^+ ions are formed in the $B^2\Sigma_u^+$ ($v' = 0$) state and that the fluorescence efficiency for the 3914-Å band is $(6.0 \pm 1.9) \times 10^{-3}$ for N_2 and $(4.8 \pm 1.5) \times 10^{-3}$ for air, in agreement with modern results at lower energies. From comparison with recent published results of primary excitation at lower energies, it appears that $\frac{2}{3}$ of the observed photons are produced by secondary electrons. Quenching cross sections for the $B^2\Sigma_u^+$ ($v' = 0$) state of N_2^+ in collisions with ground-state neutral molecules of N_2 and O_2 have been found to be $(6.5 \pm 0.4) \times 10^{-15}$ and $(10.9 \pm 4.5) \times 10^{-15}$ cm^2, respectively.

I. INTRODUCTION

We have measured the absolute fluorescence intensity of the first negative (0, 0) band of N_2^+ at 3914 Å excited by bombardment of N_2 and airlike N_2:O_2 mixtures at pressures between 0.05 and 8 Torr with electrons in the previously unstudied energy range 0.65 to 1.6 MeV. The 3914-Å photons originate from ions produced in the $B^2\Sigma_u^+$ ($v' = 0$) state by the electron-impact ionization of the ground-state N_2 molecule. Under the conditions of the experiment, ionization is produced by both the incident primary electrons and all resulting secondary electrons. From the intensity measurements, we have determined effective electron-excitation cross sections as well as quenching cross sections for the $B^2\Sigma$ state of N_2^+ in collisions

with ground-state neutral molecules of N_2 and O_2.

Knowledge of the absolute fluorescence intensity induced by relativistic electrons is important in many fields. In collision physics, excitation cross sections measured at high energies provide a definitive test for the theory of the excitation process, and help to corroborate measurements made at lower energies, as will be seen below. The behavior of the 3914-Å transition in particular affords insight into the details of the electron-impact ionization of the N_2 molecule. In geophysics, the 3914-Å band is an important feature of the auroral spectrum; a knowledge of the fluorescence *efficiency* enables one to determine the energy deposited by the primary particles producing the aurora, as well as other characteristics of the

auroral environment, from ground-based optical measurements. (The fluorescence efficiency $\eta(3914)$ is defined as the power radiated by the gas in 3914-Å photons per unit power deposited in the gas by the electron beam.)

The present work was prompted by a conflict in the literature regarding the magnitude of the 3914-Å excitation cross section. The cross sections were determined from experiments in which the incident electrons, at energies up to 60 keV, traverse a "thin" static gas sample[1-8] or neutral molecular beam,[9,10] the incident electrons losing only a small fraction of their energy to the target molecules. Those results, summarized in Fig. 1, fall into two groups, one with cross sections 2 to 3 times larger than the other; all of the measurements in the higher group have been performed since 1965.

At sufficiently high primary-electron energies, one expects the excitation cross section to follow the Born-Bethe approximation. Of the measurements described in the literature, those of Davidson and O'Neil[5] utilized the highest electron energy range. They found that, for incident electrons between 10 and 60 keV, the excitation cross section can indeed be described by the relativistic Born-Bethe approximation,

$$\sigma \,(3914 \text{ Å}) = \frac{A}{E'}\, [\ln CE' - \ln (1 - \beta^2) - \beta^2], \qquad (1)$$

where $\beta = v/c$, $E' = \frac{1}{2} m_0 \beta^2 c^2$, and v and m_0 are the velocity and rest mass of the electron. The constants A and C are given from that measurement as $A = (12.6 \pm 0.4) \times 10^{-16}$ eV cm^2 and $C = (0.08 \pm 0.04)$ eV^{-1}. The results of Schram $et\ al.$[11] for the primary-electron ionization cross section N$_2$ have the same energy dependence as the excitation cross section in (1), over the energy range 0.6 to 20 keV. Schram finds for C essentially the value given above and for the constant analogous to A a value roughly 15 times that found for excitation. From these results it can be inferred that approximately one 3914-Å photon is emitted for each 15 ionization events over the common energy range in which these expressions are valid.

Experiments have also been performed in which the electron beam is completely stopped in a thick gas target, and the resulting total photon yield is measured; from this one can evaluate an effective fluorescence efficiency which is averaged over the velocity distribution of the slowing-down electrons. Recent measurements of this type[12] yield an effective efficiency midway between those obtained from the two groups of cross section measurements shown in Fig. 1.

In addition to the unavoidable difficulties of absolute photometry, the low-energy excitation studies suffer from the same problems as those described in connection with ionization cross section
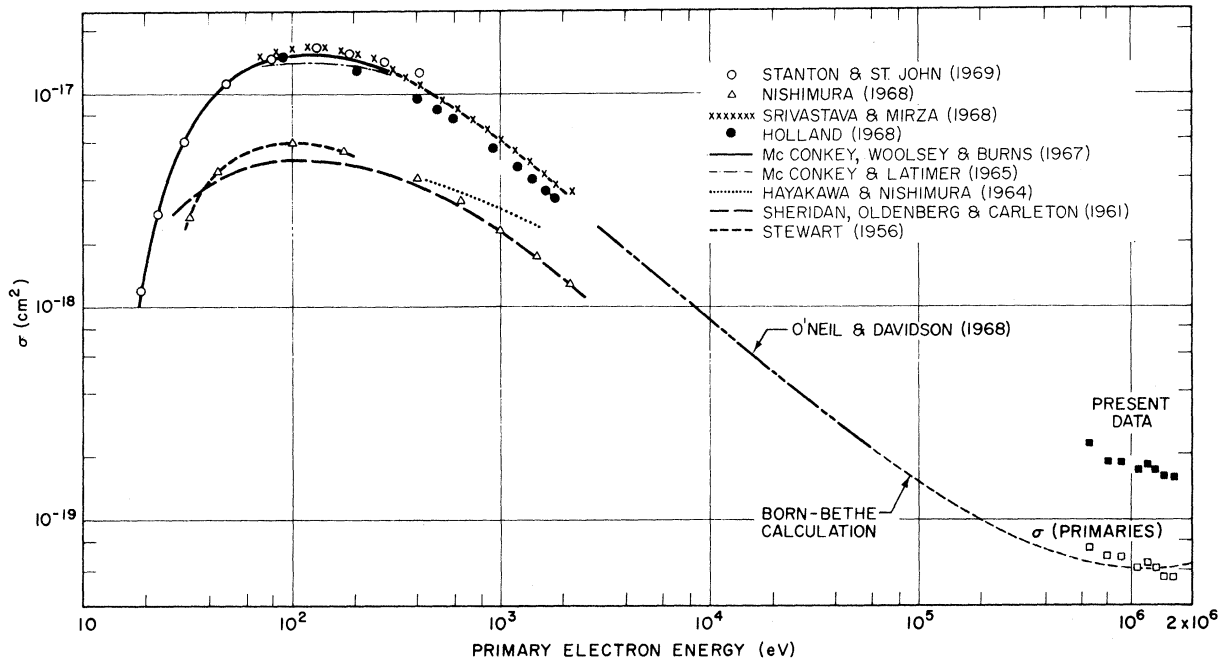
FIG. 1. Comparison of the present data at an energy around 1 MeV with those of other workers at lower energies. The dashed line is the relativistic Born approximation [Eq. (1) in the text] with the values for A and C chosen as described in Sec. IV.

measurements at those energies.[13] These include uncertainty in the actual path length of electrons in the gas, space charge and magnetic field effects, and uncertainties in the neutral density caused both by the difficulty of measuring the requisite low-gas pressures accurately and the need for apertures for the electron beam. By using electrons in the energy range around 1 MeV, we have been able to design an experiment which avoids most of these latter difficulties. In the work reported here, the electrons traverse a thin foil window (in lieu of an aperture), and impinge on a gas maintained at a pressure on the order of a few Torr. The relativistic electrons experience very little gas scattering at these pressures, and are negligibly affected by space-charge and magnetic fields present in the experiment. As a result the primary-electron paths in the gas are straight lines with a spatial distribution which is independent of gas pressure, to high accuracy. The experiment simulates the energy input found in many ionospheric situations, in which the primary particles deposit only a small fraction of their energy within a given observation region, while all resulting secondary electrons are stopped within the region.[14] Finally, the present experiment has the obvious

advantage of providing excitation cross section data in an energy range in which very little previous work has been performed.

II. DESCRIPTION OF EXPERIMENT

A diffuse beam of relativistic electrons bombards the target gas which is contained in a cylindrical chamber of 700-liter volume. The fluorescence is viewed from a long narrow truncated cone at right angles to the electron beam; this geometry minimizes such deleterious effects as wall reflections, deexcitation at the walls, and certain spatial inhomogeneities in the electron beam which would be difficult to account for analytically.

To determine the 3914-Å excitation cross section, one must measure three quantities: the density of target N_2 molecules, the flux of electrons incident on the gas, and the resulting absolute intensity in the 3914-Å band. This has been accomplished with the apparatus shown schematically in Fig. 2. Gas contained in the chamber at pressure p is bombarded by a flux of relativistic electrons of known energy and spatial distribution, producing ions, secondary electrons, and excited species. Gas densities are deduced from pressure measurements in the range 0.05–10 Torr, performed with
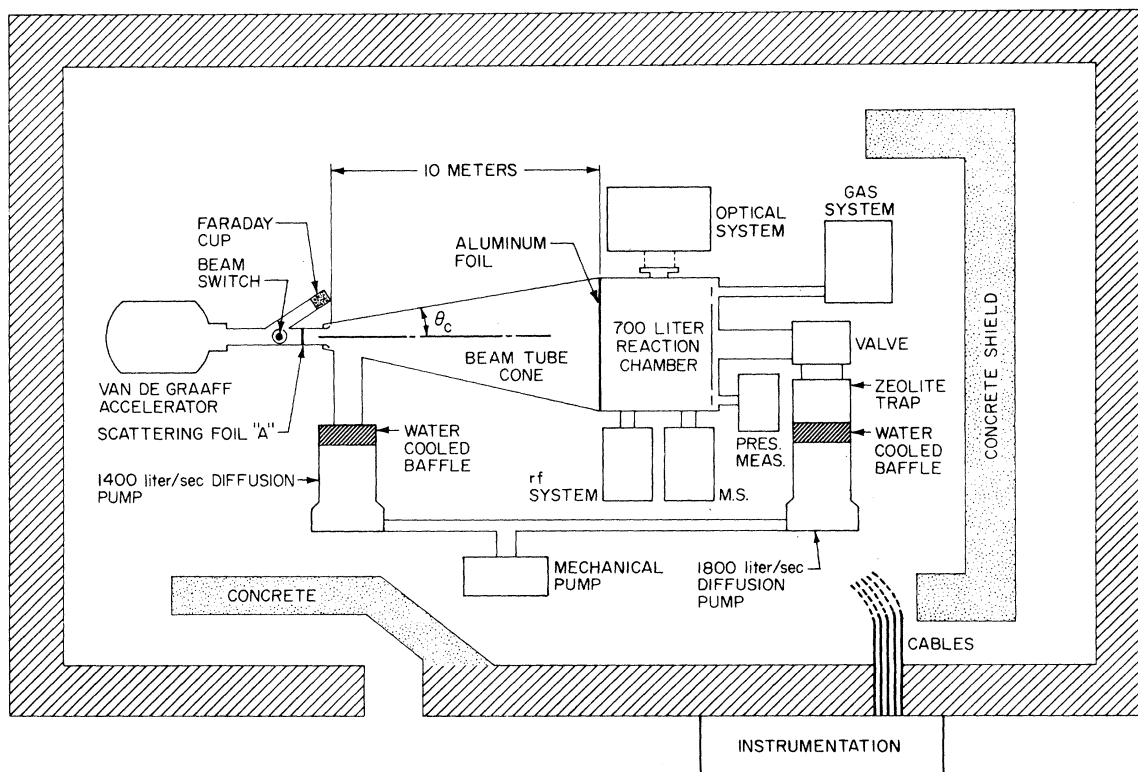
FIG. 2. Schematic diagram of the experimental system.

a capacitance manometer calibrated against a McLeod gauge. These techniques, as well as the gas handling and vacuum procedures used in this work, are described in detail elsewhere.[14]

As shown below, it also proves convenient to measure directly the total flux of electrons incident on a strip of constant width lying along the full length of the truncated cone from which the fluorescence is observed. This was accomplished by measuring the primary-electron current collected on a brass bar, 2.86 cm wide and 122 cm long, at this location. After corrections for electron reflection and secondary emission[15] these measurements yielded values in agreement with those deduced from the Faraday-cup profiles reported previously,[14] to within the accuracy of the latter, $\pm 20\%$.

The optical system is shown schematically in Fig. 3. Light from the fluorescing gas is transmitted through the quartz window, then through the collimator. The collimator consists of two circular apertures of radii $a = 1.27$ cm, $b = 0.51$ cm, separated by a distance $L = 268$ cm. The ab-

solute yield of photons in the 3914-Å band from the region of the gas defined by the collimator is measured with an interference-filter photometer as a function of electron beam flux, of electron energy between 0.65 and 1.60 MeV, and of gas pressure between 0.05 and 8.0 Torr. A scanning monochromator can be substituted for the photometer for the determination of wavelength dependences.

The interference filter used in the photometer has a peak transmission at 3916 Å, and a full width of 16.2 Å at half-maximum transmission, which effectively isolates the 3914-Å band from the remainder of the fluorescent spectrum. Figure 4 shows a low-resolution monochromator trace of the 3914-Å band seen in fluorescence from the gas with and without the interference filter; the transmission T_B of the filter for the band under all excitation conditions used is 0.135 ± 0.005, determined from the ratio of the areas under the traces.

For calibration of the photometer, a known flux of photons from a tungsten-lamp standard of spectral irradiance[16] is directed through the collimator
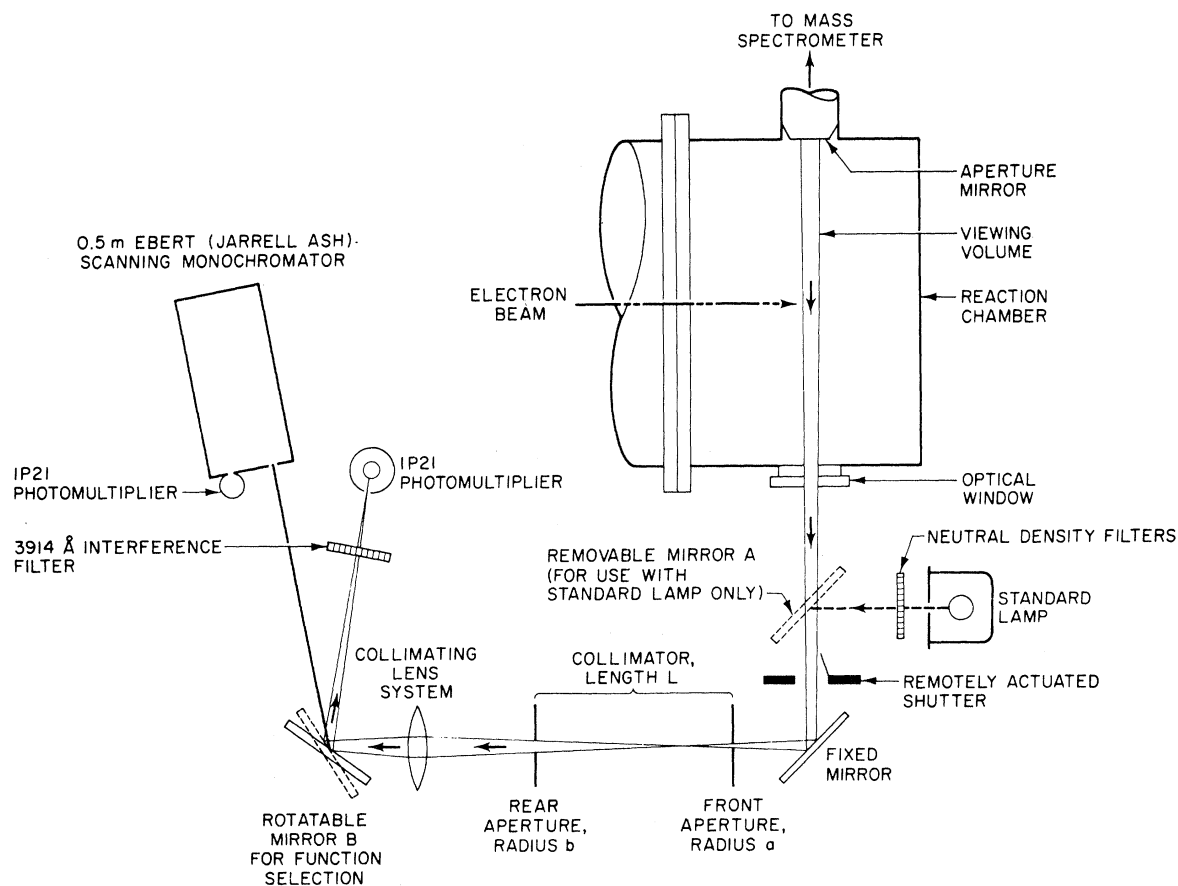
FIG. 3. Schematic diagram of the optical system.
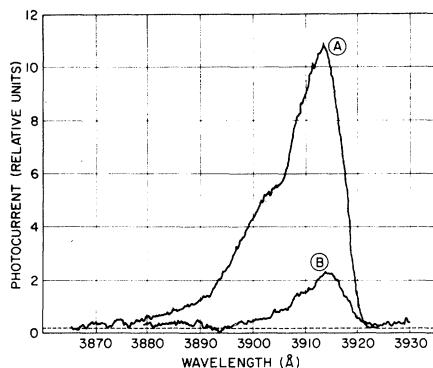
FIG. 4. Monochromator profiles of the 3914-Å band with (B) and without (A) the interference filter. The ratio of the areas under the two traces, 0.135 ± 0.005, yields the transmission of the filter for the band under the conditions of this experiment.

and into the interference-filter photometer. To avoid nonlinearities in the photomultiplier response, the standard flux is attenuated with calibrated neutral-density filters of transmission $T = (7.35 \pm 0.7) \times 10^{-5}$ to approximately the level of the 3914-Å fluorescence signal seen by the photometer. The solid angle subtended by the photometer at the standard lamp is defined by the area of the rear aperture of the collimator, which is smaller than the front aperture; all photons passing through the rear aperture reach the detector. Thus, the standard calibrating photon flux at the detector is

$$\Phi_S = \frac{W(\lambda)}{h\nu} \left(\frac{150}{L'}\right)^2 \pi b^2 R_M T_F T \ . \tag{2}$$

Here W is the power flux from the standard lamp at the desired wavelength; it is given from the supplier's calibration for 3914 Å at a distance of 150 cm from the lamp operating at the calibrated lamp current 8.30 A as $W(3914\text{Å}) = (1.37 \pm 0.04) \times 10^{11}$ eV sec^{-1} Å^{-1}. $L' = 739$ cm is the distance from the lamp to the rear aperture, a circle of radius $b = 0.51$ cm. $R_M = 0.90 \pm 0.05$ is the reflectivity of the mirror directing the standard lamp signal into the optical path, measured at 45° incidence. T_F is the integrated transmittance of the interference filter for the continuum radiation from the lamp (3.30 ± 0.10) Å. Thus the standard calibrating flux at the photomultiplier is $(3.2 \pm 0.4) \times 10^5$ photons/sec, where all of the errors are considered to be independent. This flux gives rise to a photocurrent of $(1.37 \pm 0.17) \times 10^{-8}$ A from the EMI 6256S photomultiplier when operated at the standard dynode voltage of 1025 V used for the experiment, so that the photometer sensitivity is $S = (4.3 \pm 0.5) \times 10^{-14}$ A/photon.

The fluorescing gas radiates photons in the 3914-Å band uniformly into 4π sr at the rate $\Phi(\vec{r})$ photons/sec per cm^3 of the gas. The number of photons per second dF reaching the element of area dS of the rear aperture is

$$dF = \frac{1}{4\pi} \Phi(\vec{r}) \, d\Omega \, dV, \tag{3}$$

where $d\Omega$ is the solid angle subtended by dS. The total flux at the photomultiplier is obtained by integration of Eq. (3) over the area of the rear aperture and over the viewing volume of the gas defined by the collimator.

The geometry of the gas-collimator-detector system is shown in Fig. 5. The gas is contained in the reaction chamber, bounded on one end of the optical path by a quartz window, of reflectivity R_2, and on the other by a plane mirror normal to the optic axis, of reflectivity R_1. Light from the gas traverses the window and enters the collimator, the rear aperture of which is located a distance z_0 from the window. We assume that the photon source density $\Phi(\vec{r})$ is essentially constant over a cross section of the narrow viewing region, and is a function only of position along the cavity diameter; that is

$$\Phi(\vec{r}) = \Phi(z) \ . \tag{4}$$

Then Eq. (A10) (cf. Appendix) gives for the flux of photons incident on the photometer,

$$F = \frac{\pi a^2 b^2}{4L^2} \, R \int_{z_0}^{z_1} \Phi(z) \, dz \ . \tag{5}$$

The effect of successive reflections between the mirror and the quartz window, and of the finite transmissivity of the window, is expressed in the constant R, as explained in the Appendix; for the present case we have $R = 1.88 \pm 0.04$. The fluorescence-induced photocurrent can now be expressed as

$$I = SFT_B \ , \tag{6}$$

where T_B is the transmission of the interference filter for the 3914-Å band. We now relate $\Phi(z)$ to the relevant molecular parameters.

III. ORIGIN OF THE FLUORESCENCE SIGNAL

The rate of emission of photons of frequency ν_{jk}, corresponding to a radiative transition from the molecular state E_j to E_k per cm^3 of the fluorescing gas, is

$$\Phi(\nu_{jk}) = A_{jk} N_j \ , \tag{7}$$

where N_j is the density of molecules per cm^3 in the parent state E_j of the transition, and A_{jk} is the spontaneous-emission coefficient for the transi-
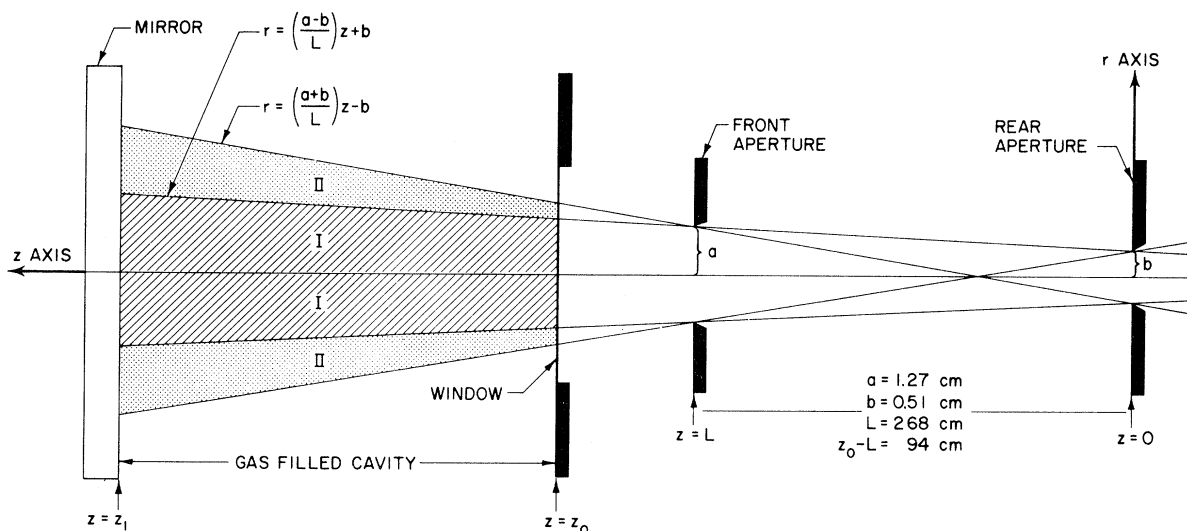
FIG. 5. Cross-sectional view of the collimation and viewing volume geometries employed for the photometer.

tion. Under the weak-excitation conditions employed in this experiment, N_j is produced by binary encounters between electrons and neutral ground-state N_2 molecules:

$$\left(\frac{\partial N_j}{\partial t}\right)_{exc} = K_j(E)p_N i(\vec{r}) . \tag{8}$$

E is the energy of the incident electrons, p_N the partial pressure of N_2 in the gas, and i ($\vec{r}$) the spatially dependent flux of beam electrons. The production coefficient can be expected to be pressure-independent for pressures sufficiently high that all secondary electrons produced in ionizing encounters of beam electrons with the gas molecules are fully stopped in the gas.[14] $K_j(E)$ is related to the cross section for excitation of the $B^2\Sigma$ state of N_2^+ by

$$\sigma_j(E) = 4.52\times10^{-30}(T/273\ °K)K_j(E) . \tag{9}$$

The $B^2\Sigma$ state is deexcited in two ways. First, the molecule can radiate spontaneously to all lower states yielding a spectrum which includes the 3914-Å band:

$$\left(\frac{\partial N_j}{\partial t}\right)_{rad} = -\sum_{k=0}^{j-1} A_{jk}N_j \equiv -A_j N_j , \tag{10}$$

where A_j is the reciprocal of the radiative lifetime of state N_j. It is convenient to introduce the "branching ratio" $B_{jk} \equiv A_{jk}/A_j$ for a given transition of N_j. The excited molecule can also lose its internal energy in collisions with other molecules; this process, known as quenching, is described by

$$\left(\frac{\partial N_j}{\partial t}\right)_{quench} = -\sum_m C_{mj}\ p_m N_j . \tag{11}$$

Here the p_m are partial pressures of the possible collision partners, and the C_{mj} their corresponding quenching coefficients. Cross sections for the quenching process can be defined from the measured C_{mj} by

$$\sigma_{mj} = \frac{C_{mj}}{\bar{v}} , \tag{12}$$

where $\bar{v}$ is the mean relative speed of the colliding molecules. In nitrogen at a total pressure p, the quenching frequency is simply $C(N_2)\ p$; for air it is $[0.8C(N_2)+0.2C(O_2)]p$. For convenience in the following equations we will use the total pressure p and an effective quenching coefficient C.

In the steady state, the production rate of N_j is equal to its total removal rate, so that

$$N_j = \frac{K_j(E)p_N i(\vec{r})}{A_j + Cp} . \tag{13}$$

Then $\Phi(\vec{r}) = A_{jk}N_j = \dfrac{B_{jk}K_j(E)p_N i(\vec{r})}{1+Cp/A_j} .$ (14)

$B_{jk}K_j(E)$ is the production coefficient for the photons in question. The small axial divergence of the beam flux permits the replacement of i ($\vec{r}$) with i (z), which justifies the approximation in Eq. (4).

From Eqs. (5), (6), and (14), we can write

$$I = ST_B \frac{\pi a^2 b^2 RB_{jk}K_j(E)p_N}{4L^2(1+Cp/A_j)} \int_{z_0}^{z_1} i(z)dz . \tag{15}$$
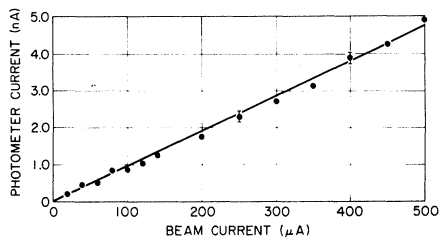
FIG. 6. Signal from the 3914-Å photometer versus electron beam current incident on N_2 at a pressure of 1.90 ± 0.05 Torr. The uncertainty in the measurement is represented by the error bars.

From Eq. (15), the quenching rate of the 3914-Å band can be determined from

$$\frac{p_N}{I} \propto A_j + Cp . \tag{16}$$

A plot of the measured values of the left-hand side of Eq. (16) versus total gas pressure should be a straight line for which the ratio of slope to intercept is C/A_j. The photon production coefficient can be evaluated in terms of the intercept $(p_N/I)_{p=0}$. Thus,

$$B_{jk}K_j(E) = \frac{4L^2}{(p_N/I)_{p=0} \, S \, T_B \, \pi a^2 b^2 R \int_{z_0}^{z_1} i(z) \, dz} . \tag{17}$$

IV. RESULTS AND DISCUSSION

Figure 6 shows a measurement of the 3914-Å fluorescence intensity in N_2 at a pressure of 1.90 ± 0.05 Torr as a function of the average current density of 1.50-MeV electrons. Linear variation of the signal with beam current density has been observed for all cases examined, over the pressure range 0.05 to 8 Torr in both N_2 and air. From this observed linearity, the $B^2\Sigma$ state must be excited from a state whose population is beam independent; only the ground state of the N_2 molecule satisfies this criterion.

In this same pressure range, however, the 3914-Å intensity is not linear with gas pressure. Figure 7 shows plots of photometer current versus total gas pressure, for both N_2 and air; the data flatten at high pressure in the manner described by Eq. (15) for collisional quenching. Figure 8 shows plots of p/I versus total gas pressure [cf. Eq. (16)] for the same data; the slope-to-intercept ratios for these straight lines are (0.95 ± 0.05) Torr^{-1} in nitrogen, (1.05 ± 0.08) Torr^{-1} in air. From these results and the measured reciprocal lifetime $A_j = (1.52 \pm 0.08) \times 10^7$ sec^{-1} for the $B^2\Sigma$ state,[17] Eq. (12) yields, for the cross section for collisional quenching of that state by
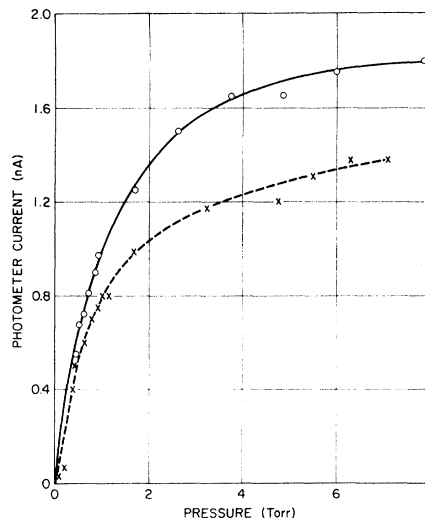
FIG. 7. Variation of intensity of the 3914-Å band with gas pressure in N_2 (o) and air (x).

ground state N_2 and O_2 molecules, the values shown in Table I; results obtained by other workers,[5,18] included for comparison, are in good agreement.

The intercepts of the p/I plots are given by

$$(p/I)_{p=0}(N_2) = (0.52 \pm 0.03) \text{ Torr/nA,}$$

$$(p/I)_{p=0}(\text{air}) = (0.63 \pm 0.05) \text{ Torr/nA.}$$

The intercepts are in the ratio 0.83 ± 0.08, which is to be compared with the expected ratio 0.80 based on the partial pressure of N_2 in air. The flux of monoenergetic electrons producing the observed glow was measured along the optic axis as described in Sec. II. Using this measurement we find the value of the integral in Eqs. (15) and (17) to be $(1.31 \pm 0.25) \times 10^{-6}$ A/cm for 1.46-MeV electrons. Then, from Eq. (17), one obtains
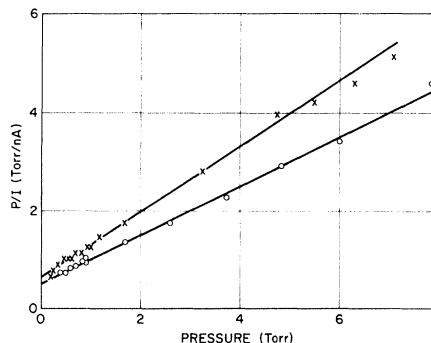
FIG. 8. 3914-Å quenching plot in N_2 (o) and air (x). The straight lines were determined by a least-squared-error fit to the data.

TABLE I. Coefficients and cross sections for quenching of 3914-Å transition of N_2^+ in collisions with ground-state N_2 and O_2 molecules $[A_j = (1.52 \pm 0.08) \times 10^7 \, \text{sec}^{-1}]$.[a]

Quenching molecule	C_j/A_j (Torr^{-1})	$\sigma_j (10^{-16} \, \text{cm}^2)$ Present work	$\sigma_j (10^{-16} \, \text{cm}^2)$ Davidson and O'Neil[b]	$\sigma_j (10^{-16} \, \text{cm}^2)$ Brocklehurst and Downing[c]
N_2	0.95 ± 0.05	65 ± 4	59 ± 14	59 ± 22
O_2	1.5 ± 0.6	109 ± 45	140 ± 100	$\cdots$

[a] Reference 17.
[b] Reference 5.
[c] Reference 18.

$$B_{jk}K_j(1.46 \, \text{MeV})$$
$$= (3.14 \pm 0.73) \times 10^{10} (\text{cm sec Torr } \mu\text{A})^{-1}.$$

From a series of measurements similar to those described above over the electron energy range 0.65 to 1.59 MeV, we have compiled the results shown in Table II for $B_{jk}K_j$, the production coefficient for 3914-Å photons by electron bombardment of ground-state N_2 molecules. Also shown in the Table is the apparent photon excitation cross section $\sigma(\text{app}) = B_{jk}\sigma_j(E)$ obtained formally from Eq. (9) for a temperature of 300 °K.

From the vibrational-transition probabilities computed by Wallace and Nicholls,[19] $B_{jk} = 0.63$; thus the coefficient for production of $B^2 \Sigma_u^+ (v' = 0)$ is given by

$$K_j(1.46 \, \text{MeV}) = (5.0 \pm 1.2) \times 10^{10} (\text{cm sec Torr } \mu\text{A})^{-1}.$$

Comparison of $B_{jk}K_j$ with the ionization rate coefficients measured previously[14] at (1.5 ± 0.1) MeV, for N_2,

$$K_{\text{ion}}(1.5 \, \text{MeV}) = (4.75 \pm 1.0) \times 10^{11} (\text{cm sec Torr } \mu\text{A})^{-1},$$

for air,

$$K_{\text{ion}}(1.5 \, \text{MeV}) = (4.93 \pm 1.0) \times 10^{11} (\text{cm sec Torr } \mu\text{A})^{-1},$$

yields the result that approximately 10% of all nitrogen ions produced by the ionizing electrons are formed in the $v' = 0$ vibrational level of the $B^2 \Sigma_u^+$ state of N_2^+. Also, approximately one 3914-Å photon is produced for every 15 electron-ion pairs.

The fluorescence efficiency $\eta(E)$ for production of 3914-Å photons by electrons of energy E can be deduced from the relationship

$$\eta(E) = \frac{B_{jk}K_j(E) h\nu p_N}{K_{\text{ion}}(E) W p} \equiv \frac{B_{jk}\sigma_j(E) h\nu p_N}{\sigma_{\text{ion}}(E) W p} \quad (18)$$

Here W, the primary energy expenditure per electron-ion pair, is 35.0 eV for N_2, 33.9 eV for air.[20,21] From the measurements described above,

we find

for N_2: $\eta(1.46 \, \text{MeV}) = (6.0 \pm 1.9) \times 10^{-3}$;

for air: $\eta(1.46 \, \text{MeV}) = (4.75 \pm 1.50) \times 10^{-3}$.

In Table III, we compare the above value for the fluorescence efficiency in air with those obtained from comparison of primary-electron excitation cross sections obtained by previous workers at lower energies with the primary ionization cross sections of Schram et al.[11] The efficiency based on our measured values for apparent excitation and ionization cross sections agrees with the higher efficiencies shown in Table III. If the larger primary excitation cross sections are indeed the correct ones, then the fluorescence efficiency is very nearly constant over the energy range from near threshold to 1.5 MeV.

In our earlier measurements in nitrogen, we observed a cross section for ionization by both primaries and all resulting secondaries which was higher by a factor of (2.8 ± 0.7) than could be attributed to the primaries alone.[14] Three pieces of evidence support this ratio: (a) Primary-electron ionization cross sections measured in the MeV range by Rieke and Prepejchal[22]; (b) Primary-electron ionization cross sections extrapolated by Eq. (1) to the MeV range from the 20-keV measurements of Schram et al.[11]; (c) Prediction of the ratio of total to primary ionization events by Bethe[23] from the original stopping-power theory. Since the production of the 3914-Å photon represents one particular channel of the ionization process, that is, the production of N_2^+ ($B^2 \Sigma_u^+$, $v' = 0$), it is reasonable to assume that this same factor of 2.8 applies to the ratio $\sigma(\text{apparent})/\sigma$ (primary) for 3914 Å fluorescence as well. Indeed, extrapolation of the primary-electron excitation cross sections of Davidson and O'Neil[5] to the MeV range by means of Eq. (1) yields primary cross sections roughly 3 times smaller than our measured total cross sections over the energy range 0.65 to 1.60

TABLE II. Production rate coefficients and effective cross sections for excitation of 3914-Å photons by collisions of electrons of energy E with N_2 molecules in the ground state.

E (MeV)	$B_{jk}K_j$ (cm sec Torr μA)$^{-1}$	σ_{app} (cm^2)
0.65	$(4.1 \pm 0.9) \times 10^{10}$	$(2.1 \pm 0.5) \times 10^{-19}$
0.80	$(3.7 \pm 0.9) \times 10^{10}$	$(1.9 \pm 0.4) \times 10^{-19}$
0.93	$(3.6 \pm 0.8) \times 10^{10}$	$(1.9 \pm 0.4) \times 10^{-19}$
1.06	$(3.3 \pm 0.8) \times 10^{10}$	$(1.7 \pm 0.4) \times 10^{-19}$
1.20	$(3.6 \pm 0.8) \times 10^{10}$	$(1.8 \pm 0.4) \times 10^{-19}$
1.33	$(3.4 \pm 0.8) \times 10^{10}$	$(1.7 \pm 0.4) \times 10^{-19}$
1.46	$(3.1 \pm 0.7) \times 10^{10}$	$(1.6 \pm 0.4) \times 10^{-19}$
1.59	$(3.1 \pm 0.7) \times 10^{10}$	$(1.6 \pm 0.4) \times 10^{-19}$

TABLE III. Comparison of the fluorescence efficiency $\eta(3914\,\text{Å})$ in air derived from the measurements of various investigators.

Workers	Energy range (eV)	Notes	$\eta\,(\times 10^{-3})$
Sheridan *et al.* (Ref. 1)	$500-3\times10^4$	a, b	2.0 ± 0.2
Stewart (Ref. 2)	$50-200$	a, c	1.7 ± 0.1
Hayakawa and Nishimura (Ref. 3)	1×10^3	a, b	2.5
Srivastava and Mirza (Ref. 4)	$600-2\times10^3$	a, b	5.0 ± 0.2
Davidson and O'Neil (Ref. 5)	$1\times10^4-6\times10^4$	a, b	4.6 ± 0.2
Holland (Ref. 6)	$100-2\times10^3$	a, b	4.8 ± 0.8
McConkey and Latimer (Ref. 9)	$30-300$	d, c	4.4 ± 0.2
McConkey *et al.* (Ref. 10)	$300-2\times10^3$	d, b	5.0 ± 0.2
	$30-300$	d, c	4.4 ± 0.4
Hartman (Ref. 12)	750	e	3.4 ± 0.2
Present work	1.5×10^6	f	4.75 ± 1.5

ᵃStatic gas target. Only primary-electron excitation significant.

ᵇExcitation cross sections were measured in pure N_2. η in air was deduced from Eq. (18) from the ionization cross sections of Schram *et al.* (see Ref. 11) for N_2 and O_2, with $p=1.25p_N$ and $W=33.9$ eV.

ᶜSame as note b except that the ionization data of D. Rapp and P. Englander-Golden, J. Chem. Phys. <u>43</u>, 1464 (1965), was used, due to the absence of data at these energies from Schram *et al.* (see Ref. 11).

ᵈCrossed-beam experiment.

ᵉStatic gas target in which primary and secondary electrons are completely stopped.

ᶠStatic gas target in which all the secondary electrons are stopped but which is a thin target for the primaries.

MeV, as shown in Fig. 1. Thus a factor of 2.8 between total and primary excitation, which is supported by our ionization measurements, brings the present data into agreement with the higher excitation cross sections measured at lower energies. To make the present data consistent with the smaller excitation cross sections, it would be necessary to ascribe to the secondary electrons about 6 times as much ionization as that produced by the primaries, which is unsupported by any other data.

V. SUMMARY OF RESULTS

Absolute measurements have been made of the production rate coefficient, effective electron excitation cross sections, and fluorescence efficiencies for the first negative (0, 0) band of N_2^+ at 3914 Å, in nitrogen and airlike $N_2{:}O_2$ mixtures. Measurements were performed for incident electrons in the energy range 0.65 to 1.6 MeV, under conditions in which the gas was a thick target for slow secondary electrons but a thin target for the primaries.

By comparison of our measured excitation coefficients with our recently reported ionization coefficients, the fluorescence efficiency for the 3914-Å band in nitrogen and air was found to be

for N_2, $\eta(1.46\ \text{MeV}) = (6.0\pm1.9)\times10^{-3}$,

for air, $\eta(1.46\ \text{MeV}) = (4.75\pm1.5)\times10^{-3}$,

in agreement with recent results obtained at lower energies by other workers; the fluorescence efficiency thus appears to be energy-independent from near threshold energy to 1.65 MeV. From this same comparison, one sees that 10% of the ions are formed in the $B^2\Sigma_u^+\,(v'=0)$ state. Two out of three of the excited states thus formed radiate into the 3914-Å band.

To relate our measured "apparent" excitation cross sections which include the contributions from secondaries as well as primaries, we have relied on the similarity of 3914-Å excitation to ionization in nitrogen. Our earlier ionization measurements under the same experimental conditions were consistent with a ratio of 2.8 between "apparent" and primary ionization cross sections. Using this same factor of 2.8 for excitation, and assuming further that the primary cross section displays the energy dependence of the relativistic Born approximation, the cross sections obtained in this work agree well with recent cross section measurements performed at energies three orders of magnitude lower. This result adds weight to the conviction already suggested by the fluorescence efficiency measurements that these recent higher cross-section results are correct.

Quenching cross sections for the $B^2\Sigma$ state of N_2^+ in collisions with ground-state neutral molecules of N_2 and O_2 have also been determined; the values

$$\sigma_{N_2}(1.46\ \text{MeV}) = (65\pm4)\times10^{-16}\ \text{cm}^2,$$

$$\sigma_{O_2}(1.46\ \text{MeV}) = (109\pm45)\times10^{-16}\ \text{cm}^2$$

are also in good agreement with the results of other workers.

ACKNOWLEDGMENTS

The authors wish to express their gratitude to Dr. Walter G. Chestnut, who originally suggested this problem. We also would like to thank David R. Maerz, who assisted in the design and construction of the apparatus, and James A. Slevin, who participated in the early measurements.

APPENDIX: EVALUATION OF INTEGRALS FOR PHOTOMETER CALIBRATION

From Eq. (3), the total flux of photons from a specified band striking the detector per unit time from the entire accessible volume of the fluorescing gas is

$$F = \frac{1}{4\pi} \int dV \int \Phi\,(\vec{r})\,d\Omega \ . \tag{A1}$$

$\Phi(\vec{r})$ is the photon flux at the wavelength of interest into 4π steradians per unit volume of the gas per second. Equation (A1) is integrated over the volume of the gas seen by the detector, and over the solid angle subtended by the detector for each volume element.

Figure 5 is a cross section (in the r-z plane) of the two apertures, the window, and the cavity region seen by the detector. The collimating apertures divide the viewing volume into a central region I, in which each volume element has an unobstructed view of the rear aperture, and the penumbral region II, in which the front aperture partially blocks the view of the rear aperture. We treat the two regions separately, then combine the results at the end of the calculation. As explained in the text, all photons passing through the rear aperture are detected, so that the detector integration can be performed over the area of the rear aperture. The photon source term $\Phi(\vec{r})$ is approximated by $\Phi(z)$, where z is the coordinate along the optical path, which is coincident with the chamber diameter. Initially we neglect reflections from the mirror or optical window, as well as the finite transmission through the window; these will be included later.

The coordinate system is shown in Fig. 9. Here $\vec{r}_0$ lies in the plane of the rear aperture ($z = 0$) and $\vec{r}$ lies in the plane $z =$ constant. The solid angle subtended at the point P in the gas by the element of surface dS on the rear aperture is

$$d\Omega = \frac{\cos\theta}{D^2}\ dS = \frac{z\,dS}{D^3}\ , \tag{A2}$$

where θ is the angle between D and the normal to dS. Since in our case $|\vec{r} - \vec{r}_0|^2 \leqslant 10^{-4} z^2$, D can be replaced by z in Eq. (A2).

Each volume element in Region I, which extends from the optic axis $r = 0$, to $r = b + [(a - b)/L]\,z$, has an unobstructed view of the full rear aperture.
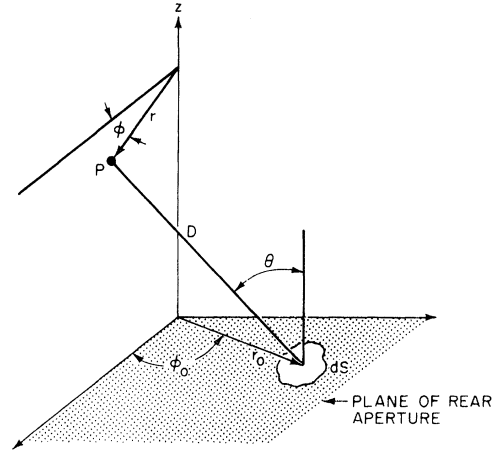
FIG. 9. Coordinate system used for integration.

Thus for Region I, Eq. (A1) becomes

$$F_1 = \frac{1}{4\pi} \int dV \int \frac{\Phi(z)}{z^2}\ dS$$

$$= \frac{1}{4\pi} \int dS \int_0^{2\pi} d\phi \int_{z_0}^{z_1} dz \int_0^{b + (\frac{a-b}{L})z} \Phi(z)z^{-2}\,r\,dr$$

$$= \frac{\pi b^2}{4} \int_{z_0}^{z_1} \Phi(z)\left[\frac{b}{z} + \frac{a-b}{L}\right]^2 dz \ . \tag{A3}$$

In Region II, bounded by $r = b + (a - b)/L\ z$ and $r = [(a + b)/L]\,z - b$, the surface integral over the rear aperture depends on the coordinates (r, z) of the emitting volume element in the gas, as shown in Fig. 10. Now the integration is performed over that portion of the area of the rear aperture intercepted by the cone with apex at r, z. Since the front and rear apertures lie in parallel planes, the projection of the circular front aperture from r, z onto the plane of the rear aperture is itself a circle of radius $az/(z - L)$ centered at $rL/(z - L)$. In terms of the coordinates displayed in Fig. 11, we find

$$\int dS \equiv S'(r') = \theta_0 b^2 + R^2\theta - \tfrac{1}{2}[(2br')^2 - (b^2 - R^2 + r'^2)^2]^{1/2} . \tag{A4}$$

Here $R = az/(z - L)$ and $r' = rL/(z - L)$. Then

$$F_2 = \frac{1}{4\pi} \int_0^{2\pi} d\phi \int_{z_0}^{z_1} dz \int_{b + (\frac{a-b}{L})z}^{(\frac{a+b}{L})z - b} \Phi(z)S'(r')rz^{-2}\,dr \ . \tag{A5}$$

Expressing (A5) in terms of r' rather than r, we find after some simple manipulations

$$F_2 = \frac{1}{2L^2} \int_{z_0}^{z_1} \Phi(z)\left(\frac{z-L}{z}\right)^2 dz \int_{R-b}^{R+b} S'(r')r'\,dr' . \tag{A6}$$
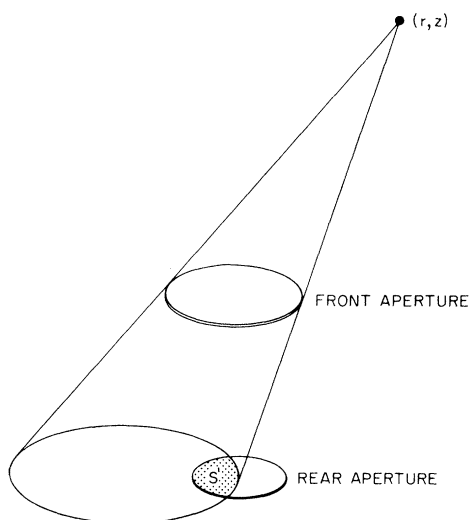
FIG. 10. Three-dimensional view of a light cone from the penumbral region. Only that light from (r, z) which passes through the shaded area S' is detected.

The r' integration yields, after much manipulation,

$$\int_{R-b}^{R+b} S'(r')r' dr' = \tfrac{1}{2}\pi b^3 (2R - b) = \tfrac{1}{2}\pi b^3 \left(\frac{2az}{z-L} - b \right).$$

$$(A7)$$

Substitution into Eq. (A6) yields

$$F_2 = \frac{\pi}{4} \frac{b^3}{L^2} \int_{z_0}^{z_1} \Phi(z) \left(\frac{z-L}{z} \right)^2 \left[\frac{2az}{z-L} - b \right] dz . \quad (A8)$$

Combining Eqs. (A3) and (A8), we obtain

$$F = \frac{\pi a^2 b^2}{4L^2} \int_{z_0}^{z_1} \Phi(z) dz . \quad (A9)$$

This result permits the following simple treatment of the reflection of light from the mirror and window. Figure 5 shows the mirror opposite the window; light initially travelling away from the photometer can be reflected into the collimator from the mirror. In effect, the mirror reflects the cavity volume into an image space behind the mirror, in which the viewing volume can be found by extending the surfaces defining Regions I and II into the image space. The image space can be treated as a "gas" fluorescing with a source intensity Φ $(z)R_1$, where R_1 is the reflectivity of the mirror for 3914 Å photons. Subsequent reflections from the window of reflectivity R_2, back into the mirror, etc., can be treated in an analogous manner, as shown in Figure 12. This leads directly to the result

$$F = \frac{\pi a^2 b^2}{4L^2} R \int_{z_0}^{z_1} \Phi(z) dz , \quad (A10)$$

where

$$R = (1 + R_1 + R_1 R_2 + R_1^2 R_2 + R_1^2 R_2^2 + \cdots)(1 - R_2) .$$

The factor $1 - R_2$ accounts for reflection losses experienced by all the photons in traversing the window. We measured $R_1 = 0.90 \pm 0.04$; $R_2 = 0.07$ computed from the refractive index; then numerically $R = 1.88 \pm 0.04$.

FIG. 11. Notation and detailed geometry used for the region II integration.
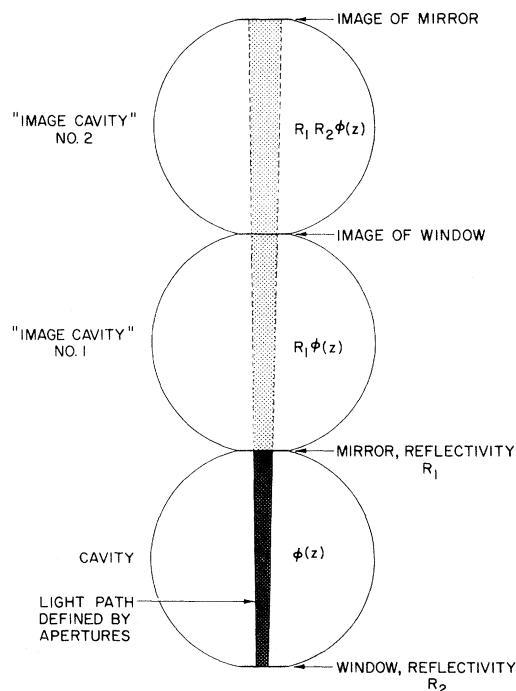
FIG. 12. Schematic illustration of the reflection calculation.

*Work supported by Defense Atomic Support Agency, under NWER Subtask HC061, contract No. DASA-01-67-C-0089.

[1]W. F. Sheridan, O. Oldenberg, and N. P. Carleton, in *Abstracts of the Second International Conference on the Physics of Electronic and Atomic Collisions, Boulder, Colo.* (W. A. Benjamin, New York, 1961).

[2]D. T. Stewart, Proc. Phys. Soc. (London) A69, 437 (1956).

[3]S. Hayakawa and H. Nishimura, J. Geomag. and Geoelect. (Japan) 16, 72 (1964).

[4]B. N. Srivastava and I. M. Mirza, Phys. Rev. 168, 86 (1968).

[5]G. Davidson and R. O'Neil, American Science and Engineering, Inc., Report No. AFCRL-67-0277, Cambridge, Mass., 1968 (unpublished).

[6]R. F. Holland, LASL Report No. LA-3783, 1968 (unpublished).

[7]P. N. Stanton and R. M. St. John, J. Opt. Soc. Am. 59, 252 (1969).

[8]H. Nishimura, J. Phys. Soc. Japan 24, 130 (1968).

[9]J. W. McConkey and I. D. Latimer, Proc. Phys. Soc. (London) 86, 463 (1965).

[10]J. W. McConkey, J. M. Woolsey, and D. J. Burns, Planet. Space Sci. 15, 1332 (1967).

[11]B. L. Schram, F. J. de Heer, M. J. van der Viel, and J. Kistemaker, Physica 31, 94 (1964).

[12]P. L. Hartman, LASL Report No. LA-3793, 1968 (unpublished).

[13]L. J. Kieffer and G. H. Dunn, Rev. Mod. Phys. 38, 1 (1966).

[14]M. N. Hirsh, P. N. Eisner, and J. Slevin, Phys. Rev. 178, 175 (1969); Rev. Sci. Instr. 39, 1547 (1968).

[15]J. G. Trump and R. J. Van de Graaff, Phys. Rev. 75, 44 (1949).

[16]The lamp used was a tungsten-iodine spectral irradiance standard, serial number EPI-1173, Eppley Laboratory, Inc., Providence, R.I.

[17]R. G. Bennet and F. W. Dalby, J. Chem. Phys. 31, 434 (1959).

[18]B. Brocklehurst and F. A. Downing, J. Chem. Phys. 46, 2976 (1967).

[19]L. V. Wallace and R. W. Nicholls, J. Atmos. Terr. Phys. 7, 101 (1955).

[20]J. M. Valentine and S. C. Curran, Repts. Progr. Phys. 21, 1 (1958).

[21]W. P. Jesse, Phys. Rev. 109, 2002 (1958).

[22]F. F. Ricke and W. Prepejchal, ANL Rad. Phys. Div. Annual Report No. ANL-7360, 1966 (unpublished).

[23]H. Bethe, Ann. Physik 5, 325 (1930).

Cesium Resonant Total Charge-Transfer Cross Section and Oscillatory Structure *

Julius Perel and Howard L. Daley
Electro-Optical Systems, Pasadena, California 91107

and

Francis J. Smith
Department of Applied Mathematics and Theoretical Physics, The Queens University of Belfast, Belfast, Northern Ireland

A more detailed measurement and calculation are reported for the $Cs^+ + Cs$ charge-transfer cross section which contains continuous uniform oscillatory structure. Ten oscillation maxima are experimentally observed in the energy range from 0.6 to 21 keV. The oscillations are regular with inverse velocity and appear to show two superimposed oscillation frequencies. Calculations suggest that this may be due to the combined effect of a maximum in the interaction potential difference and of a large repulsive electron core, each generating a separate oscillation. It is shown that there is a very wide range of different potentials which could explain the oscillations.

INTRODUCTION

Several measurements of the Cs resonant total charge-transfer cross section have been made during the past decade with most of the results reported in literature in fairly good agreement. The earlier measurements[1-4] show the typical smooth variation of the resonant cross section (σ) with the relative velocity given by $\sigma^{1/2} = A - B \ln v$. More recent measurements show this cross section to contain oscillatory structure.[5,6]

Smith[7] subsequently showed that such oscillations can result from a stationary phase effect if the difference between the gerade and ungerade phase shifts passes through a maximum. This may occur in either of two ways: the interaction potential difference may pass through a maximum (potential maximum oscillations)[7] or the two potentials may have a strong repulsive core (core oscillations).[8] Oscillations resulting from a maximum were obtained in the calculations of Peek